STUDY ON STIFFNESS OF CYLINDRICAL ROLLER BEARINGS UNDER COMBINED RADIAL AND MOMENT LOADS

[1]VAN-CANH TONG, [2]SEONG-WOOK HONG

Department of Mechanical System Engineering Kumoh National Institute of Technology, Korea
E-mail: swhong@kumoh.ac.kr

Abstract- This study investigated the effect of combined radial and moment loads on the stiffness of cylindrical roller bearings (CRBs). First, a general four degrees of freedom CRB model was presented that was applicable for a wide range of loading, radial clearance, and rotational speed. The model provided a fully-occupied stiffness matrix, the contact load between rolling elements and races, and inner ring displacements. Model verification was made by comparing the estimated bearing stiffness under pure radial load with that from a commercial program. Then, simulations were performed for the CRB under various radial and moment loads. Analysis of bearing performance was carried out with an emphasis on the bearing stiffness behavior under the effects of combined loading. Numerical results showed that, without moment load, the bearing stiffness increases with the increase of radial loading. The combined radial and moment loads introduced a nonlinear stiffness behavior. However, this nonlinearity tended to reduce with increasing moment load.

Index Terms- Combined loads, cylindrical roller bearing, displacement, simulation, stiffness.

I. INTRODUCTION

Rolling bearings have been widely used to support the loads and convert the sliding into rolling friction for reducing the power loss of the industrial machines. CRBs are frequently adopted for high-load applications such as machine tools, turbine engines, gearboxes, etc. The stiffness of bearing has a great influence on the dynamic behavior of the rotating systems such as vibration, natural frequency, and noise.

A large number of studies have been conducted to analyze the effect of bearing stiffness on the system behavior [1-5]. There are several formulae available for bearing stiffness calculations [6-8]. However, the stiffness of bearing is generally nonlinear with respect to bearing loading and other operating conditions. Thus, it cannot be simply assigned as a constant value for a wide range of loading or rotational speed. Consequently, analyzing the dependence of bearing stiffness on loading is necessary that makes possible to predict the performance of rotating system accurately. In addition, the available stiffness formulae were commonly restricted to the radial and axial stiffness coefficients. In fact, stiffness of bearing appears in a matrix form, in which either diagonal or off-diagonal stiffness elements may have certain influence on overall performance of the system. In particular, off-diagonal stiffness element that couples the radial load with the angular displacement was found to significantly modify the natural frequency of a system with ball bearings [9].

This study investigates the effect of combined radial and moment loads on the CRB stiffness. All the stiffness elements of the CRB are obtained via a four degrees of freedom bearing model, which includes the centrifugal loading and radial clearance. Then the study is extended to analyze the bearing displacement behavior. The obtained results are thoroughly discussed.

II. CRB MODEL

A. Assumptions

Several assumptions are made in this study to simplify the analysis: 1) the friction forces at all contacts are negligible; 2) the effect of lubricant film thickness is ignored; and 3) the structural deformation of bearing races is not considered, but only local deformations at rollers and race contacts are taken into account.

B. Model description

A substantial number of the CRB models have been introduced in recent studies [10-12]. This section briefly summarizes the elaboration of this model, which is used for the stiffness calculation. The CRB can freely move in the axial direction and rotate around its axis. Therefore, only four degrees of freedom model is needed as shown in Figure 1(a). Under an external load vector {F}, the inner ring is displaced from its original position by a displacement vector {δ}. The external load and displacement vectors of inner ring are written by, respectively.

$$\{F\} = \{F_x \quad F_y \quad M_x \quad M_y\}^T \qquad (1)$$

$$\{\delta\} = \{\delta_x \quad \delta_y \quad \gamma_x \quad \gamma_y\}^T \qquad (2)$$

Figure 1(b) shows the inner ring cross-section at a roller of location angle ϕ. The inner ring and roller displacement vectors are described by {u} and {v}, respectively.

$$\{u\} = \{u_r \quad \theta\}^T \qquad (3)$$

$$\{v\} = \{v_r \quad \psi\}^T \qquad (4)$$

Vector {u} can be calculated as a function of inner ring displacement {δ} by

$$\{u\} = [R_\phi]\{\delta\} \qquad (5)$$

where $[R_\phi]$ is the transformation matrix. Assume that there is no axial installation error i.e., the inner and outer ring centers are coincided, matrix $[R_\phi]$ is then given by

$$[R_\phi] = \begin{bmatrix} \cos\phi & \sin\phi & 0 & 0 \\ 0 & 0 & -\sin\phi & \cos\phi \end{bmatrix} \qquad (6)$$

Figure 1(c) illustrates a free-body diagram of a roller. The contact loads and moments between the roller and races are $Q_{i,e}$, and $M_{i,e}$, respectively, where i and e indicate inner and outer races. These contact loads are calculated using the slicing technique [11] as a function of radial clearance, roller and inner ring cross-section displacements. The roller centrifugal load F_c can be calculated as described in Ref. [12] by

$$F_c = \frac{1}{2} m d_m \omega_m^2 \qquad (7)$$

where m and d_m indicate roller mass and bearing pitch diameter, respectively. ω_m is the angular velocity of roller about its own axis. Then the equilibrium equations for the roller are obtained as follows:

$$\begin{Bmatrix} Q_i - Q_e + F_c \\ M_i - M_e \end{Bmatrix} = \begin{Bmatrix} 0 \\ 0 \end{Bmatrix} \qquad (8)$$

Solving equations (8) will give the roller displacements and the final contact loads, which, in turn, gives the equilibrium equations of the inner ring by

$$\{F\} + \sum_{j=1}^{Z} [R_\phi]^T \{Q\}_j = \{0\} \qquad (9)$$

where Z is the number of rollers. The inner ring contact load at a roller j is given by

$$\{Q\} = \{-Q_i \quad -M_i\}^T \qquad (10)$$

By solving equations (9), the inner ring displacement $\{\delta\}$ can be found. Then taking derivative of the load vector with respect to the displacement vector, the bearing stiffness matrix is obtained as

$$[k] = \left[\frac{\partial\{F\}}{\partial\{\delta\}^T}\right] = \begin{bmatrix} k_{xx} & k_{xy} & k_{x\theta_x} & k_{x\theta_y} \\ k_{yx} & k_{yy} & k_{y\theta_x} & k_{y\theta_y} \\ k_{\theta_x x} & k_{\theta_x y} & k_{\theta_x\theta_x} & k_{\theta_x\theta_y} \\ k_{\theta_y x} & k_{\theta_y y} & k_{\theta_y\theta_x} & k_{\theta_y\theta_y} \end{bmatrix} \qquad (11)$$

To calculate the stiffness matrix based on equation (11) requires several mathematical operations. Details of these calculations can be found in Refs. [10-12]. In addition, because the roller and inner ring equilibrium equations are all nonlinear, this study uses an iterative Newton-Raphson method.

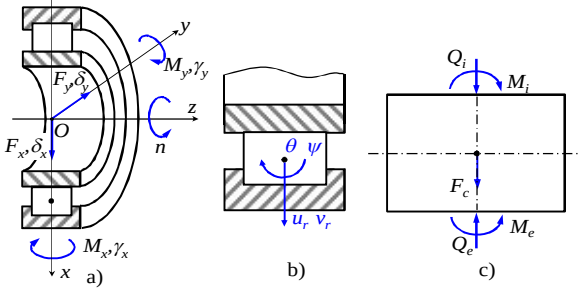


Fig.1. CRB model: a) CRB with external loads and displacements, b) cross-section of bearing at a roller, c) free-body diagram of a roller.

Table1: Parameters of the sample CRB NU1014

Parameter	Value	Parameter	Value
Bore diameter (*mm*)	70.0	Roller diameter (*mm*)	10.0
Outer diameter (*mm*)	110.0	Roller length (*mm*)	9.4
Pitch diameter (*mm*)	90.0	Number of rollers	23
Width (*mm*)	20.0		

III. RESULTS AND DISCUSSION

The above analysis is applied for a sample CRB NU1014 with basic parameters given in Table 1. The rotational speed and radial clearance of CRB are kept constant throughout the paper at n = 5000 rpm, and ε = 5 μm, respectively. All the numerical calculations are performed using MATLAB®.

C. Model verification

To verify the presented bearing model, calculated stiffness elements of the CRB are compared with those obtained from a commercial program [13]. Four diagonal stiffness elements are compared as shown in Figure 2, which shows an excellent match between the stiffness elements of current model and those from the commercial code. Therefore, it can be concluded that the present CRB model is sufficiently accurate.

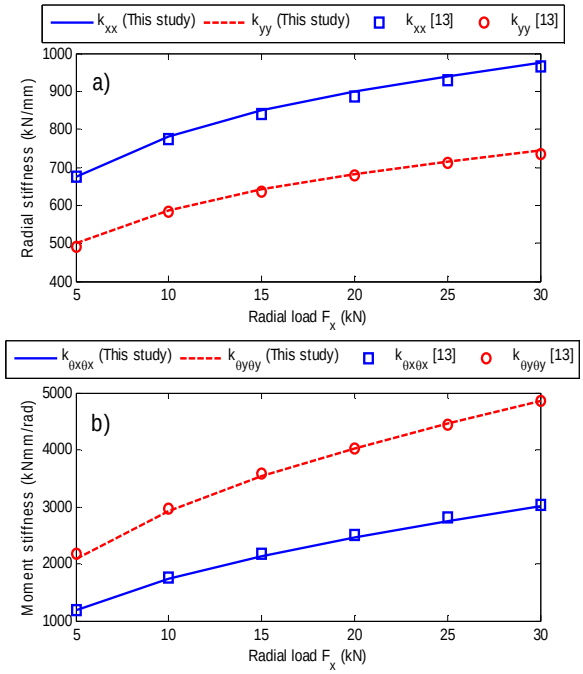
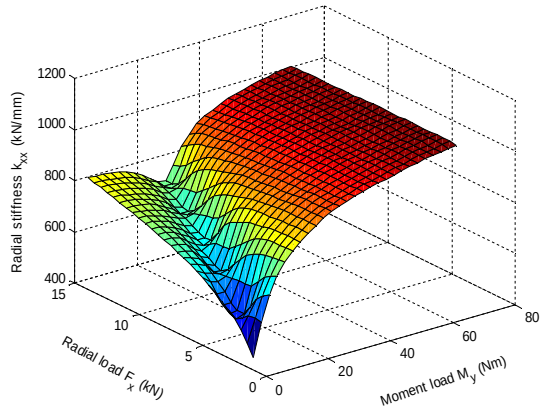


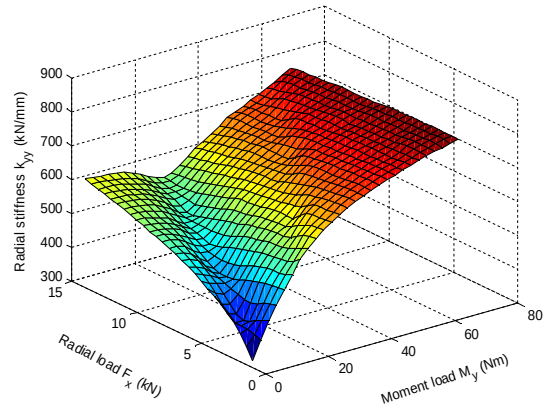
Fig.2. CRB stiffness estimated by current model and the commercial code [13]: a) radial stiffness, b) moment stiffness.

D. Effect of combined radial and moment loads

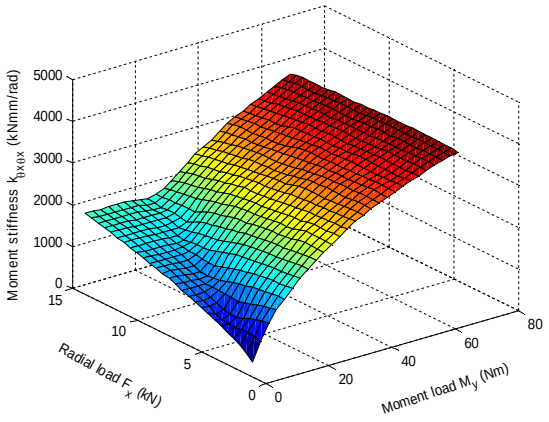
Further calculations are performed for the bearing radial load F_x varying from 1 to 14 kN, and moment load M_y varying from 0 to 65 Nm. Only the diagonal stiffness elements are evaluated, which have major effects on the dynamics of rotor-bearing systems. The obtained stiffness coefficients are demonstrated in Figure 3. Figure 4 depicts the bearing radial and angular displacements as a function of the radial and moment loads.



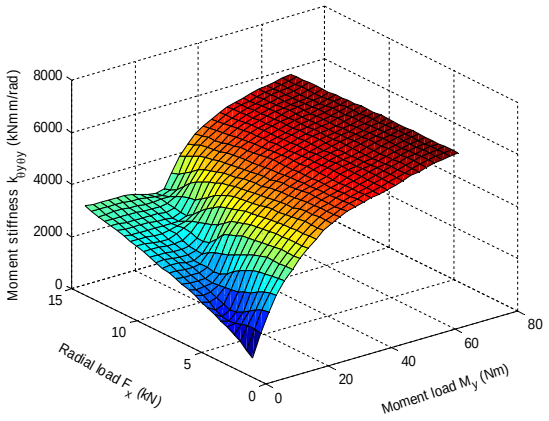
a)



b)

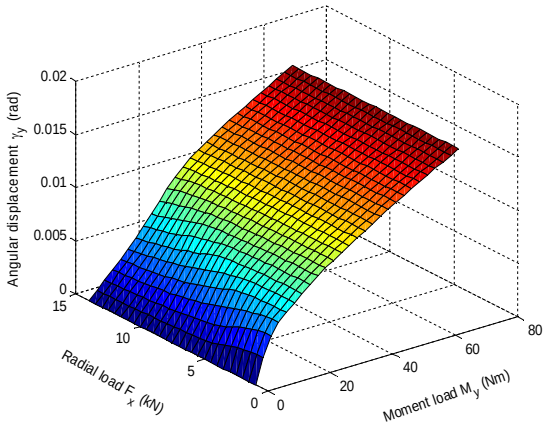


c)

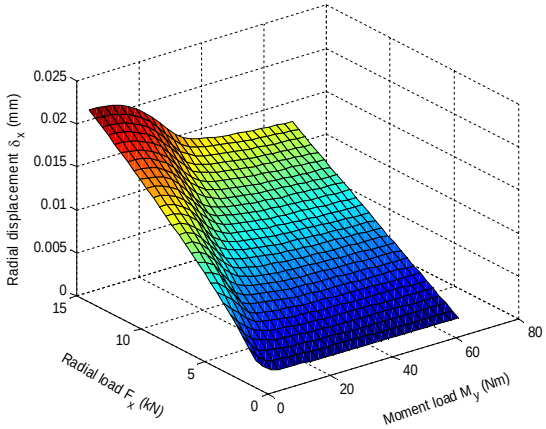


d)

Fig.3. CRB stiffness as a function of radial and moment loads: a) radial stiffness k_{xx}, b) radial stiffness k_{yy}, c) moment stiffness $k_{\theta x \theta x}$, d) moment stiffness $k_{\theta y \theta y}$.



a)



b)

Fig.4. CRB displacements as a function of radial and moment loads: a) angular displacement, b) radial displacement.

Figure 3 shows that, without moment load, all the stiffness elements increase with increasing radial load. As moment load increases, the bearing stiffness elements decrease to reach a local minimum at a certain moment load. However, beyond this value, the bearing rigidity steadily increases with the increase of moment load. This is because, for a radially loaded CRB under zero or small moment load, only half of inner ring contacts with the rollers. When the moment load increases, the contact condition recovers in most rolling elements because of increased bearing angular displacement as shown in Figure 4(a).

The radial displacement of bearing illustrated in Figure 4(b) shows that, with high moment load, the radial displacement and radial load show an approximately linear relationship. This is because under high moment load, the CRB stiffness coefficients are almost unchanged with respect to radial load as shown in Figure 3.

CONCLUSIONS

A general CRB model for stiffness and displacement calculations has been presented and verified. The stiffness behavior of CRB under combined radial and moment loads was studied. Conclusions of this study are drawn as follows:

1. Under zero moment load, the CRB stiffness increases with the increase of radial load.
2. The combined radial and moment loading introduces a nonlinear behavior in the stiffness of CRB. This nonlinearity is reduced with increasing moment load.
3. Owing to providing a fully-occupied stiffness matrix, the present bearing model is useful for further static and dynamic analysis of rotor system containing CRBs.

ACKNOWLEDGMENTS

This research was supported by the Korea Institute of Machinery and Materials.

REFERENCES

[1] T. C. Lim, and R. Singh, "Vibration transmission through rolling element bearings, Part I: Bearing stiffness formulation," Journal of Sound and Vibration, vol. 139, no. 2, pp. 179-199, 1990.
[2] Y. Guo, and R. G. Parker, "Stiffness matrix calculation of rolling element bearings using a finite element/contact mechanics model," Mechanism and Machine Theory, vol. 51, pp. 32–45, 2012.
[3] D. Noel, M. Ritou, B. Furet, and L. S. Loch, "Complete analytical expression of the stiffness matrix of angular contact ball bearings," Journal of Tribology, vol. 135, no. 4, pp. 041101, 2013.
[4] A. Gunduz, and R. Singh, "Stiffness matrix formulation for double row angular contact ball bearings: analytical development and validation," Journal of Sound and Vibration, vol. 332, no. 22, pp. 5898–5916, 2013.
[5] V. C. Tong, and S. W. Hong, "Characteristics of tapered roller bearing subjected to combined radial and moment loads," International Journal of Precision Engineering and Manufacturing-Green Technology, vol. 1, no. 4, pp. 323-328, 2014.
[6] E.P. Gargiulo, "A simple way to estimate bearing stiffness," Machine Design, vol. 52, no. 17, pp. 107–110, 1980.
[7] F. P. Wardle, S. J. Lacey, and S. Y. Poon, "Dynamic and static characteristics of a wide speed range machine tool spindle," Precision Engineering, vol. 5, no. 41 pp. 175–183, 1983.
[8] T. A. Harris, "Rolling bearing analysis," 4th ed., Wiley-Interscience, 2000.
[9] A. Gunduz, J. T. Dreyer, and R. Singh, "Effect of bearing preloads on the modal characteristics of a shaft-bearing assembly: Experiments on double row angular contact ball bearings," Mechanical Systems and Signal Processing, vol. 31, pp. 176–195, 2012.
[10] V. C. Tong, S. W. Kwon, and S. W. Hong, "Fatigue life of cylindrical roller bearings," Proceedings of the Institution of Mechanical Engineers, Part J: Journal of Engineering Tribology, 2016 (in press).
[11] J. M. de Mul, J. M. Vree, and D. A. Maas, "Equilibrium and associated load distribution in ball and roller bearings loaded in five degrees of freedom while neglecting friction–parts I, II," Journal of Tribology, vol. 111, no. 1, pp. 142-155, 1989.
[12] V. C. Tong, and S. W. Hong, "Fatigue life of tapered roller bearing subject to angular misalignment," Proceedings of the Institution of Mechanical Engineers, Part C: Journal of Mechanical Engineering Science, vol. 230, no. 2, pp. 147-158, 2016.
[13] Schaeffler Technologies, BEARINX®-online Shaft Calculation, http://www.schaeffler.de/content.schaeffler.de/en/products_services/inafagproducts/calculating/bearinxonline/bearinx_online.jsp (accessed date: Nov 03, 2016).

★★★